Supporting Information for

Symmetry-Breaking Charge Separation in a Nanoscale Terrylenediimide Guanine-Quadruplex Assembly

Natalia E. Powers-Riggs,[1] Xiaobing Zuo,[2] Ryan M. Young,[1] Michael R. Wasielewski[1]*

[1] Department of Chemistry and Institute for Sustainability and Energy at Northwestern, Northwestern University, Evanston IL 60208

[2] X-ray Science Division, Argonne National Laboratory, Lemont, IL, USA 60439

Contents

Synthesis

The syntheses of molecules **Boc$_3$GTDI** and **GTDI** are outlined below. Boc-protected N9-octyl guanine (Boc$_3$GBr) was synthesized according to established route.[1] BocGBr was then coupled to ethynyl terrylenediimide (ETDI) yielded the Boc-protected precursor (**Boc$_3$GTDI**), and protecting groups were removed with acid to yield the final **GTDI** product.

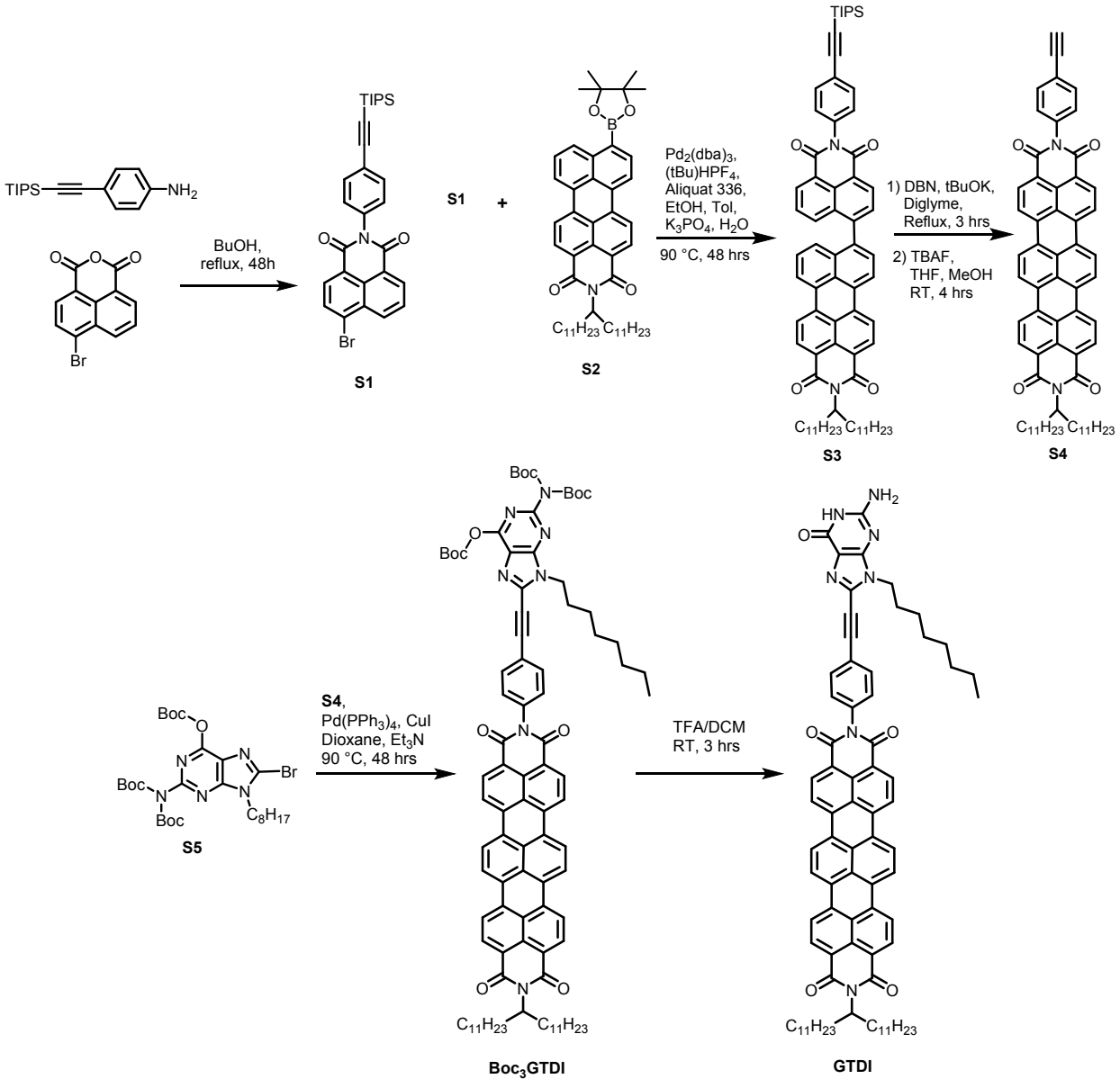

Scheme 1: Synthesis of **GTDI**.

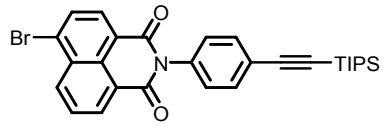

Synthesis of S1

A solution of 4-bromo-1,8-napthalenedicarboxylic anhydride (1.5 g, 6.5 mmol), 4-((triisopropylsilyl)ethynyl)aniline (2.0 g, 7.25 mmol) in tertbutyl alcohol (40 mL) was degassed and stirred at reflux for 48 hours. The mixture was cooled and solvent removed by evaporation, remaining solid purified through column chromatography (1:2 hexanes:dichloromethane) to yield **S1** (636 mg, 18%). ^{1}H NMR (500 MHz, Chloroform-*d*) δ 8.71 (dd, *J* = 7.3, 1.1 Hz, 1H,), 8.65 (dd, *J* = 8.5, 1.2 Hz, 1H), 8.46 (d, *J* = 7.8 Hz, 1H), 8.09 (d, *J* = 7.9 Hz, 1H), 7.89 (dd, *J* = 8.5, 7.3 Hz, 1H), 7.64 (d, *J* = 7.8 Hz, 2H), 7.26 (d, *J* = 7.8 Hz, 2H), 1.14 (d, *J* = 1.6 Hz, 21H).

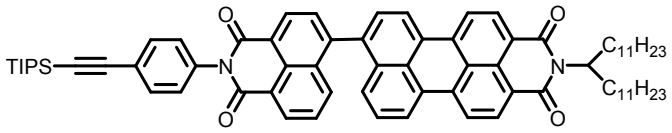

Synthesis of S3

A mixture of **S1** (478 mg, 0.9 mmol), **S2 (PMI-Bpin)** (350 mg, 0.45 mmol), Aliquat 336 (2 drops), ethanol (1 mL), and toluene (10 mL) was degassed and to was combined with $Pd_2(dba)_3$ (33 mg, 36 μmol),Tri-tert-butyl phosphonium tetrafluoroborate (20 mg, 72 μmol) and a solution of K_3PO_4 (477 mg, 2.25 mmol) in 1.3 mL deoxygenated water. The mixture was heated at 90 °C for 48 h with vigorous stirring. After cooling down to room temperature, the resulting mixture was extracted with dichloromethane (100 mL) twice, and the organic layer was dried over $NaSO_4$. The organic solvent was concentrated in reduced pressure to yield a red solid. The pure **S3** (500 mg, 100%) was obtained by silica gel column chromatography (2:1 dichloromethane/hexane). ^{1}H NMR (500 MHz, Chloroform-*d*) *δ* = 8.80 (d, *J* = 7.4 Hz, 1H), 8.71 – 8.60 (m, 4H), 8.55 (d, *J* = 8.2 Hz,

1H), 8.51 (dd, *J* = 8.1, 2.3 Hz, 2H), 7.92 (dd, *J* = 8.5, 1.2 Hz, 1H), 7.87 (d, *J* = 7.4 Hz, 1H), 7.71 – 7.63 (m, 4H), 7.51 (t, *J* = 7.9 Hz, 1H), 7.41 (d, *J* = 8.4 Hz, 1H), 7.35 – 7.30 (m, 2H), 5.21 (dt, *J* = 9.4, 3.9 Hz, 1H), 2.30 – 2.22 (m, 2H), 1.90 – 1.82 (m, 2H), 1.36 – 1.23 (m, 36H), 1.16 (s, 21H), 0.85 (t, *J* = 7.0 Hz, 6H).

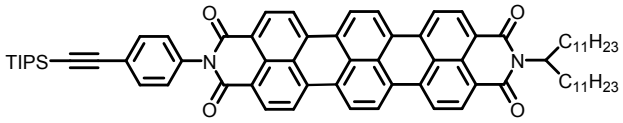

Synthesis of S3.5

A solution of **S3** (150 mg, 0.136 mmol), 1,5-Diazabicyclo[4.3.0]non-5-ene (.41 mL), Potassium Tert-butoxide (.3 mg, 3 μmol) in diglyme (0.34 mL) was prepared under nitrogen. The solution was heated to 130 °C for 3 hours. After the solution cooled, the reaction mixture was poured into water, filtered, and the resulting solid was purified through silica column chromatography to produce **S3.5** (70 mL, 47%). ^{1}H NMR (500 MHz, Chloroform-*d*) δ 8.61 (d, *J* = 8.0 Hz, 4H), 8.51 (s, 4H), 8.44 (dd, *J* = 8.3, 3.0 Hz, 4H), 7.71 – 7.64 (d, *J* = 8.0 Hz, 2H), 7.37 – 7.30 (d, *J* = 8.0 Hz, 2H), 5.24 – 5.13 (m, 1H), 2.27 (m, 1H), 1.89 (m, 2H), 1.32 – 1.18 (m, 36H), 1.17 (d, *J* = 1.4 Hz, 21H), 0.84 (t, *J* = 6.9 Hz, 6H).

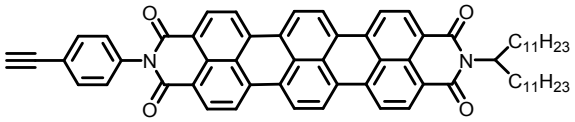

Synthesis of S4

The product (25 mg, 23 μmol) was then dissolved in tetrahydrofuran (5 mL) and methanol (1mL), cooled to 0 °C and to it was mixed tetra-n-butylammonium fluoride on SiO_2 (16 mg, 25 μmol). The mixture was warmed to room temperature over the course of 30 minutes, and stirred for an

additional 4 hours. The solvent was evaporated and the reaction mixture was purified through column chromatography (100% DCM → 1% THF) to yield **S4** (8 mg, 37%).

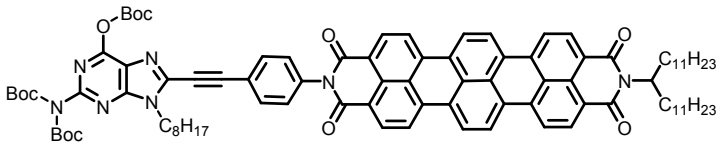

Synthesis of Boc$_3$GTDI

A solution of **S4** (20 mg, 21 μmol) and **S5** (Boc$_3$GBr) (20 mg, 32 μmol) in anhydrous dioxane (5 mL) and triethylamine (2 mL) was purged with N_2, and to it was added $Pd(PPh_3)_4$ (3 mg, 1 μmol) and CuI (1 mg, 2 μmol). The air-free solution was stirred at 90 C for 48 hours, when it became a homogenous blue solution. The solution was cooled, solvents were evaporated, and the solid was washed with methanol to remove any unreacted **S5**. The remaining solid was purified through column chromatography ($CHCl_3$ → 1% THF) to produce **Boc$_3$GTDI** (11 mg, 35%). ^{1}H NMR (500 MHz, Chloroform-*d*) δ 8.72 – 8.41 (m, 12H), 7.81 (d, *J* = 8.1 Hz, 2H), 7.45 (d, *J* = 8.1 Hz, 2H) 5.20 (dq, *J* = 9.3, 4.5, 3.3 Hz, 1H), 4.40 (t, *J* = 7.0 Hz, 2H), 1.74 (s, 9H), 1.41 (s, 18H), 1.34 – 1.18 (s, 46H), 0.87 (t, *J* = 7.0 Hz, 3H), 0.83 (t, *J* = 7.0 Hz, 6H).

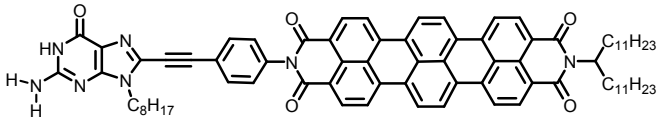

Synthesis of GTDI

To a 5mL solution of 4:1 dichloromethane:trifluoroacetic Acid was added 20 mg **Boc$_3$GTDI**. The solution was stirred at room temperature for 1 hour then slowly quenched with methanol. Reaction contents were filtered, washed with methanol and purified through column chromatography

($CHCl_3$, 1% THF → 5% MeOH). ^{1}H NMR (600 MHz, DMSO-d_6, 100°C) δ 10.47 (s, 1H), 8.59 (d, *J* = 9.1 Hz, 8H), 8.42 (d, *J* = 7.8 Hz, 2H), 8.36 (d, *J* = 7.6 Hz, 2H), 7.76 (d, *J* = 8.0 Hz, 2H), 7.53 (d, *J* = 7.9 Hz, 2H), 6.38 (s, 2H), 5.12 – 5.04 (m, 1H), 4.14 (t, *J* = 7.2 Hz, 2H), 2.19 (d, *J* = 9.0 Hz, 2H), 1.88 (s, 4H), 1.38 (s, 4H), 1.32 – 1.22 (m, 20H), 1.18 (d, *J* = 13.1 Hz, 22H), 0.86 (t, *J* = 6.6 Hz, 3H), 0.78 (t, *J* = 7.0 Hz, 6H).

X-ray Scattering Analysis

Samples were prepared in 3 x 10^{-3} M concentration solutions of THF, followed by sonication for 20 minutes. Larger aggregates or undissolved material was removed by passing samples through a 0.2 μm syringe filter.

All small-/wide-angle X-ray scattering (SAXS/WAXS) were collected at beamline 12-ID-B of the Advanced Photon Source at Argonne National Laboratory. Solution samples were injected through a flow cell of (2 mm path length) with a syringe pump set up to flow the samples and reduce X-ray radiation damage. All samples were exposed to the 13.3 keV X-ray source through 30 scans of 1 second each. SAXS data were collected on a Pilatus 2M detector, allowing for detection q range of 0.0035-0.9 $Å^{-1}$ and a Pilatus 300K detector for WAXS data, for detection up to 2.5 $Å^{-1}$.

Scattering intensity is reported as a function of the modulus of the scattering vector q, related to the scattering angle 2θ by the equation $q = (4\pi/\lambda) \sin \theta$, where λ is the X-ray wavelength. Solvent scattering intensity was subtracted from the sample data. Further analysis was conducted using the ATSAS package.[2]

Structures were designed in Avogadro,[3] and scattering simulated with Crysol.[4] Models with and without alkyl tails were modeled, a structure including the $C_{23}H_{47}$ aliphatic chain off the TDI and the octyl tail on the guanine provided the best fit.

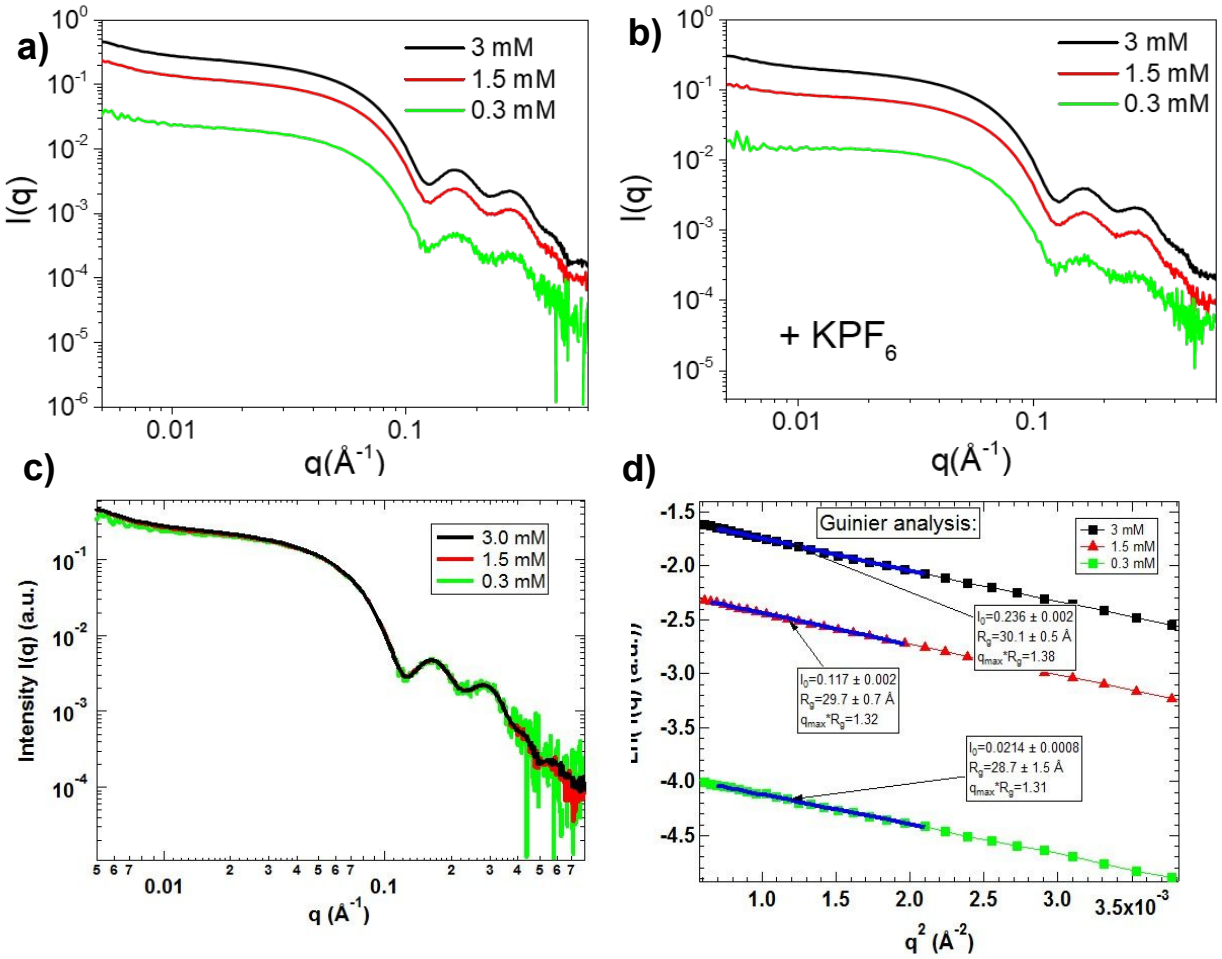

Figure S1: Background-subtracted SAXS profiles for samples of **GTDI** at various concentrations in THF a) neat, b) with the addition of 0.25 eq KPF_6 salt. c) superimposition of SAXS data for neat **GTDI** in a. d) Guinier plots for SAXS data for neat **GTDI** in a.

The SAXS data in Figure S1a, c-d suggest that **GTDI** forms a nearly monodisperse assembly at 0.3-3.0 mM concentrations for the following reasons. First, the SAXS data produce good linear Guinier plots, which indicates that either one assembly species/size dominates or a limited number of assemblies with comparable sizes and comparable concentrations are present. Second, the SAXS profiles for samples of 0.3-3.0 mM superimpose well. The slightly discrepancy in the q range below 0.06 $Å^{-1}$ arises from concentration effects or/and weak inter-particle interactions. Simulations of the data in Figure S2a show that the SAXS profiles in the q range of 0.05 - 0.5 $Å^{-1}$ change significantly when the **GTDI** assembly size changes from 3 to 18 layers. If there were

multiple assembly species in the solution under SAXS study, i.e., $(\mathbf{GTDI_4})_n$ layers, $(\mathbf{GTDI_4})_{n+1}$ layers, $(\mathbf{GTDI_4})_{n+2}$ layers,..., it would mean that there was a dynamic equilibrium among those species. Increasing **GTDI** concentration from 0.3 mM to 3 mM (one order of magnitude) would most likely drive the equilibrium significantly toward larger assemblies, therefore the SAXS profile of the sample would be the summation of contributions from all species, and would change along with the **GTDI** concentration. However, the three SAXS profiles in Figure S1c, are virtually identical in the q range of 0.06 - 0.6 $Å^{-1}$ when superimposed, which indicates the assembly composition remains unchanged when increasing from 0.3-3.0 mM. Therefore, the SAXS data suggest there is one dominant species/particle size for concentrations of 0.3-3.0 mM.

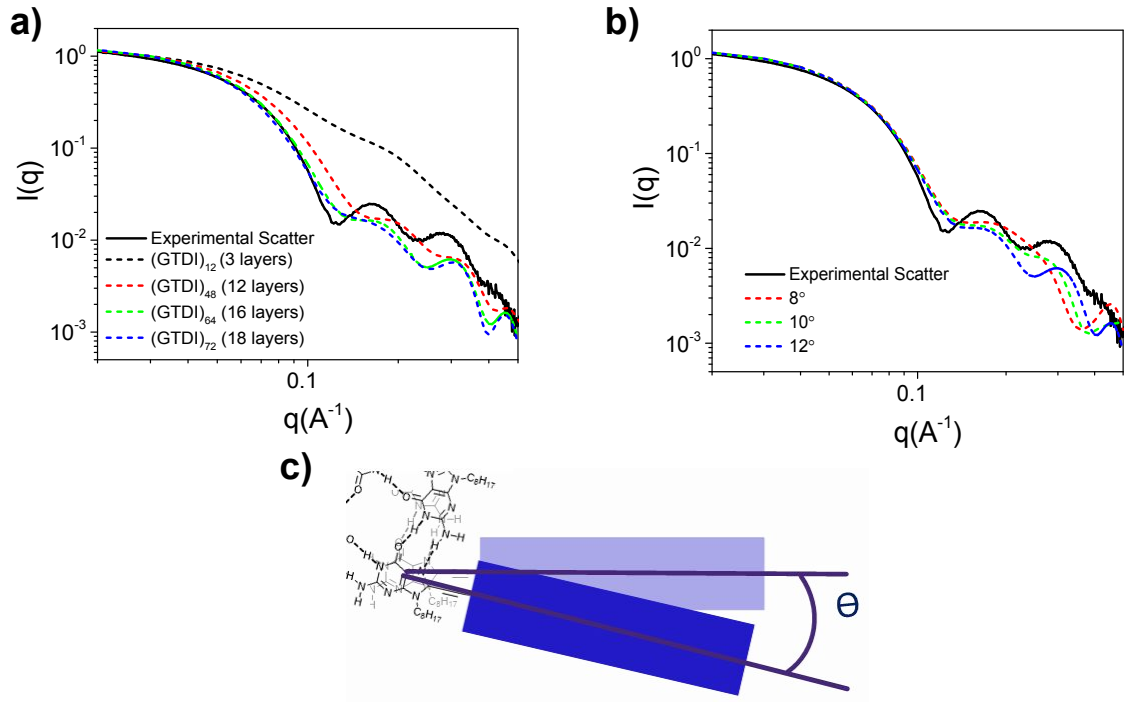

Figure S2: Comparisons of **GTDI** experimental scattering profiles with simulated scatter of proposed structural models a) GQ assemblies of variable size with rotational offset set at 12°, b) GQ assemblies of **$(GTDI_4)_{16}$** with varying rotational offset angle, c) depiction of offset angle measurement.

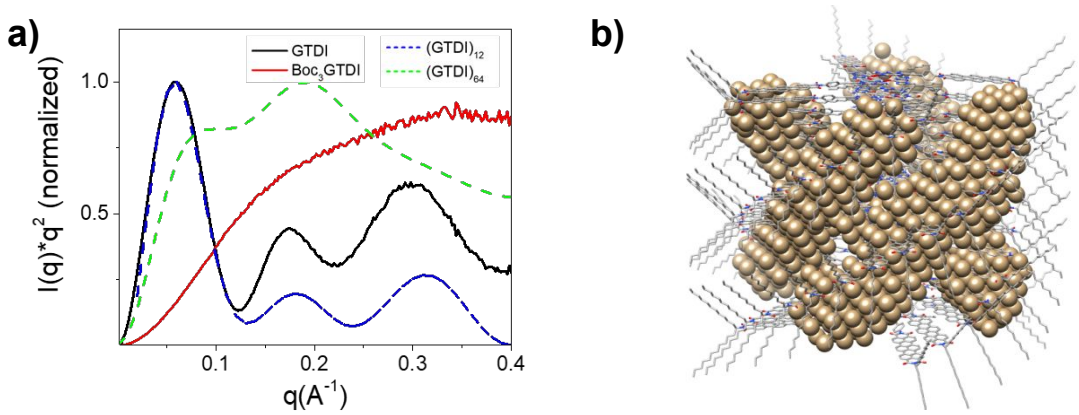

Figure S3: Comparisons of experimental data of 3 x 10^{-3} M **GTDI** (black) and **Boc_3GTDI** samples (red), with models of G-quadruplex structures made of 3 layers (dashed green) and 16 layers (dashed blue) in a Kratky plot. b) Overlay of simulated bead-model and proposed structure model.

Table S1: Comparison of real and proposed *Rg* values from Guinier and PDF analyses

	Guinier R_g (Å)	PDDF R_g (Å)
GTDI (3 x 10^{-3} M)	30.1 ± 0.5	27.9
$(GTDI)_{64}$	29.6	28.5

Forward Scattering of GTDI and Boc_3GTDI

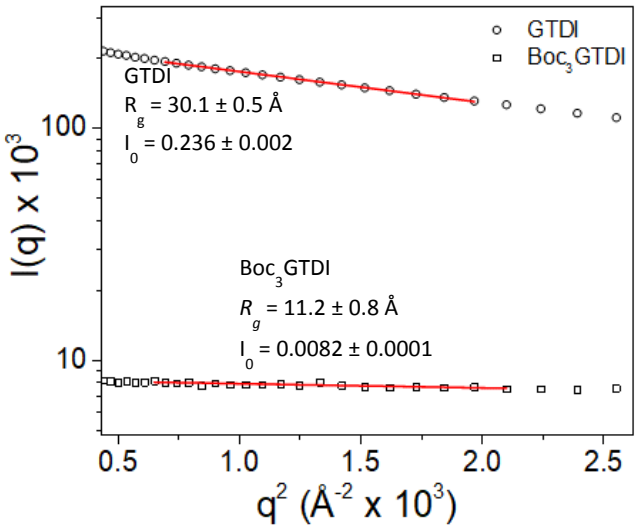

Figure S4: Guinier fits of 3 mM solution of **GTDI** and **Boc_3GTDI** in THF.

Forward scattering value scales with molecular weight of aggregates. **GTDI** forward scattering values indicate aggregates with roughly 28 times the molecular weight of **Boc_3GTDI** aggregates. Adjusting for differences in mass, aggregates of **GTDI** contain 35 more molecules than **Boc_3GTDI**. If we assume that the average aggregate in 3 mM **Boc_3GTDI** THF solution is 2 units large, this supports the claim that **GTDI** aggregates into structures consisting of 16 quartets, or 64 moieties in total.

Steady-State Spectroscopy

Samples were prepared with anhydrous THF purified on a Glass Contour solvent system. Spectra were obtained at room temperature on a Shimadzu 1800 UV-vis spectrometer, NIR absorption data were obtained on a Shimadzu 3600 UV-vis spectrometer. Emission spectra were collected on a Horiba Nanolog fluorimeter with a perpendicular arrangement of the excitation source and detector. All emission spectra were corrected for monochromator wavelength dependence and CCD-detector spectral response functions. Integration times of 5 s were used to record spectra of the complexed TDI solutions. Fluorescence quantum yields were determined using cresyl violet perchlorate in methanol as a standard.

Steady-state UV-vis absorption spectroscopy

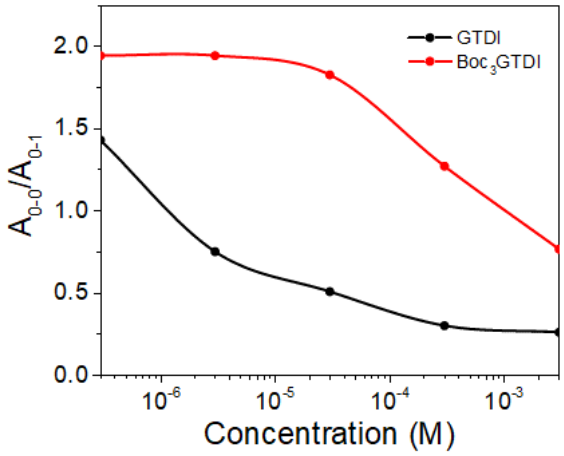

Figure S5: Ratio of relative intensities of 0-0 and 0-1 transitions for **Boc$_3$GTDI** and **GTDI** steady-state absorption.

Steady-state emission

The **GTDI** emission spectrum is substantially broadened and red-shifted with respect to the dilute monomeric TDI emission spectrum (Figure S4). In contrast, concentrated **Boc$_3$GTDI** displays a largely monomeric emission signal, with a shoulder at 800 nm suggestive of aggregation. The **GTDI** sample is largely non-fluorescent, with fluorescence quantum yields estimated to be < 0.01, compared to Φ_{FL} = 0.098 for 3 x 10^{-3} M samples of **Boc$_3$GTDI**.

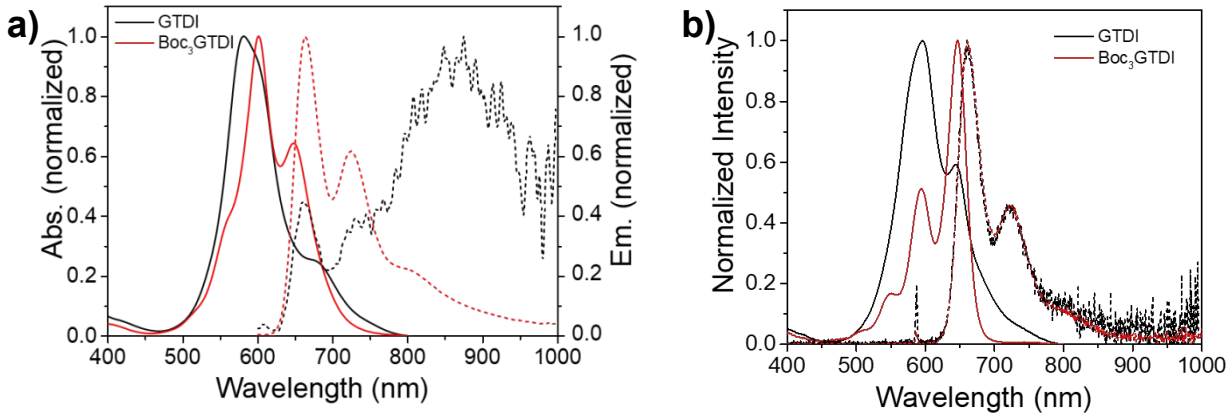

Figure S6: Normalized absorption (full line) and emission (dashed line) spectra of **GTDI** and **Boc$_3$GTDI** at concentrations of a) 3 × 10-3 M and b) 3 × 10^{-6} M.

Infrared spectroscopy

Fourier-Transform Infrared spectroscopy (FTIR) was performed on high concentration (3 x 10^{-3} M) samples of **Boc$_3$GTDI** and **GTDI** in THF-d_8 (Fig SX). Peaks corresponding to C=C modes at 1586 cm^{-1}, and C=O modes at 1654 and 1694 cm^{-1} were observed for both compounds, and are in good agreement with published absorption for TDI.[5] Spectra of bare and Boc-protected guanine acetylene demonstrates peaks at 1600, 1760, and 1800 cm^{-1} in **Boc$_3$GTDI** and 1678 cm^{-1} in **GTDI** are largely not due to TDI contributions.

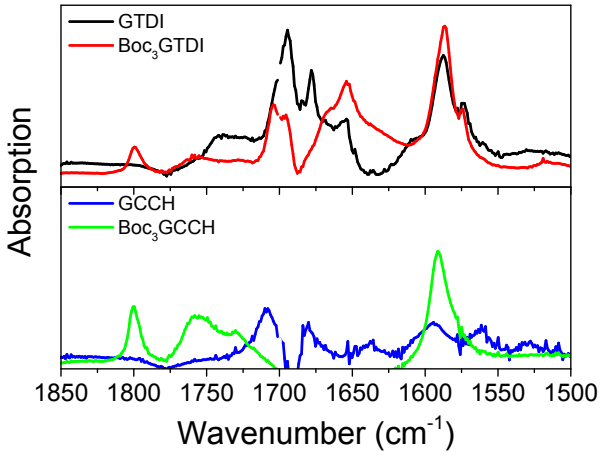

Figure S7: FTIR spectra of **GTDI** and **Boc$_3$GTDI** (top) and guanine acetylene and Boc-protected guanine acetylene reference (bottom).

Chemical Reduction of GTDI

Sample Preparation

Cobaltocene ($CoCp_2$), was purchased from Sigma-Aldrich and stored in an N_2 glovebox. All experiments were performed in anhydrous CH_2Cl_2 solutions, previously degassed, in a glovebox under an N_2 atmosphere. UV/Vis absorbance spectra were recorded in an air-free quartz cell with an optical path-length of 2 mm containing the solution of interest. Samples were prepared immediately prior to use.

GTDI was prepared in a 3 x 10^{-3} M solution of CH_2Cl_2, then diluted to 3 x 10-5. GTDI displays the same aggregated stead-state absorption spectrum as 3 mM THF across all measured concentrations.

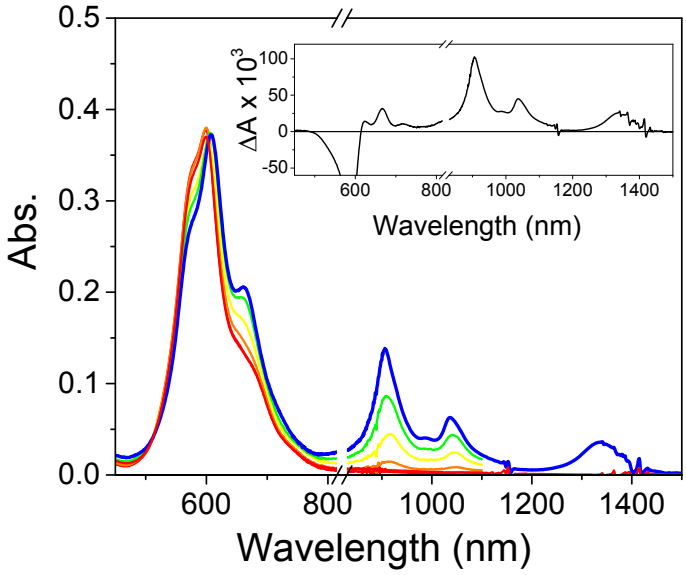

Figure S8: Vis/NIR absorption of **GTDI** in CH_2Cl_2 with the addition of cobaltocene. Inset shows difference spectrum of partially reduced **GTDI** and neutral **GTDI** solution.

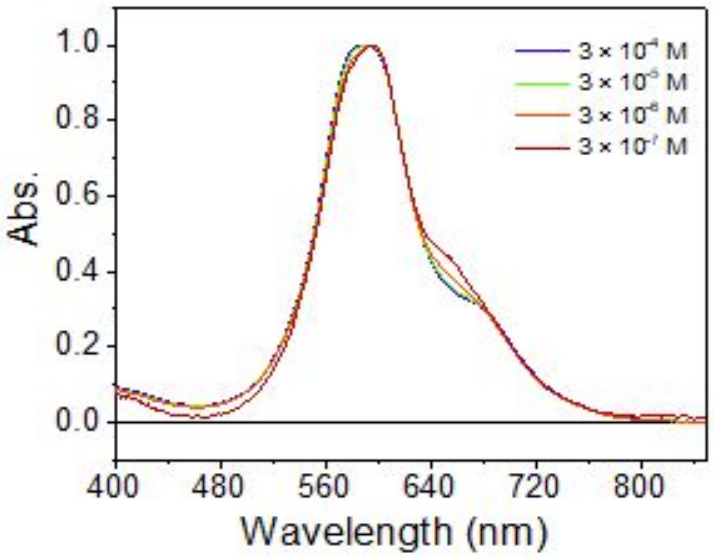

Figure S9: Normalized absorption spectra of GTDI in CH_2Cl_2.

Time-Resolved Optical Spectroscopy

Sample Preparation

Dilute concentration (3 x 10^{-6} M) **GTDI** sample was prepared in a glass cuvette with 2 mm pathlength and an OD of 0.1 at λ_{max}. Concentrated **GTDI** and **Boc$_3$GTDI** (3 x 10^{-3} M) samples were prepared in demountable cells (Harrick Scientific, Inc) with 25 μm pathlength and 0.5 OD at λ_{max}.

Visible and Near-Infrared Transient Absorption Spectroscopy

Femtosecond visible and near-infrared (fsTA) spectroscopy experiments were performed using a regeneratively-amplified Ti:sapphire laser system (Tsunami oscillator / Spitfire Pro amplifier, Spectra-Physics) as previously described,[6] and the excitation pulses were generated with a home-built optical parametric amplifier. The samples were irradiated at λ_{ex} = 585 nm with ~110 fs, 0.6 μJ pulses that were depolarized (DPU-25-A, Thorlabs, Inc) to suppress observation of rotational dynamics. Transient spectra were acquired with 4 s averaging at each time delay point. The instrument response was about 300 fs.

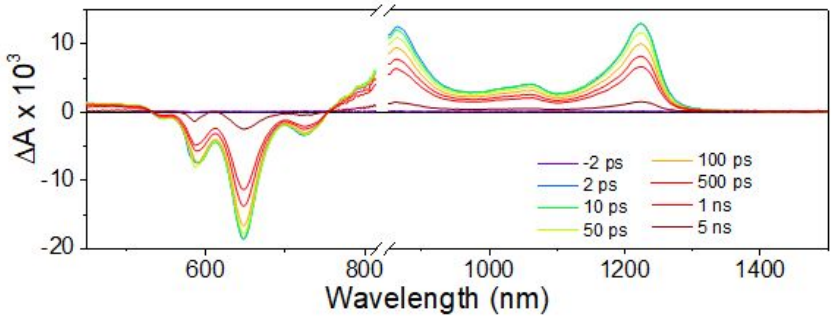

Figure S10: fsTA spectrum of **Boc$_3$GTDI** in 3 x 10^{-6} M THF.

Data Processing / Fitting for Time-Resolved Optical Spectroscopy

Data Treatment

Femtosecond Spectroscopy: Prior to kinetic analysis, the fsTA data are background/scatter-subtracted and chirp-corrected, and the visible and NIR data sets are spectrally merged (Surface Xplorer 4, Ultrafast Systems, LLC).

Global Analysis

The kinetic analysis was performed using home written programs in MATLAB[7] and was based on a global fit to selected single-wavelength kinetics. The time-resolution is given as w = 300 fs (full width at half maximum, FWHM); the assumption of a uniform instrument response across the frequency domain and a fixed time-zero (t_0) are implicit in global analysis.

Multiple-Wavelength Global Fitting

The kinetic data from multiple different wavelengths are fit using the global analysis described below. Each wavelength is given an initial amplitude that is representative of the spectral intensity at time t_0, and varied independently to fit the data. The time/rate constants and t_0 are shared between the various kinetic data and are varied globally across the kinetic data in order to fit the model(s) described below.

Species-Associated Fitting

We globally fit the dataset to a specified kinetic model and use the resultant populations to deconvolute the dataset and reconstruct species-associated spectra.

1st order model:

We use a first-order kinetic model with rate matrix K:

$$\underline{K} = \begin{pmatrix} -k1 & 0 & 0 \\ k1 & -k2 & 0 \\ 0 & k2 & k3 \end{pmatrix} \qquad \text{(Eqn. S1)}$$

The MATLAB program numerically the solves the differential equations through matrix methods,[8] then convolutes the solutions with a Gaussian instrument response function with width *w* (FWHM), before employing a least-squares fitting using a Levenberg-Marquardt or Simplex method to find the parameters which result in matches to the kinetic data.

Spectral Reconstruction

Once the fit parameters are established, they are fed directly into the differential equations, which were solved for the populations of the states in model—i.e., A(t), B(t), and C(t). Finally, the raw data matrix (with all the raw data) is deconvoluted with the populations as functions of time to produce the spectra associated with each species.

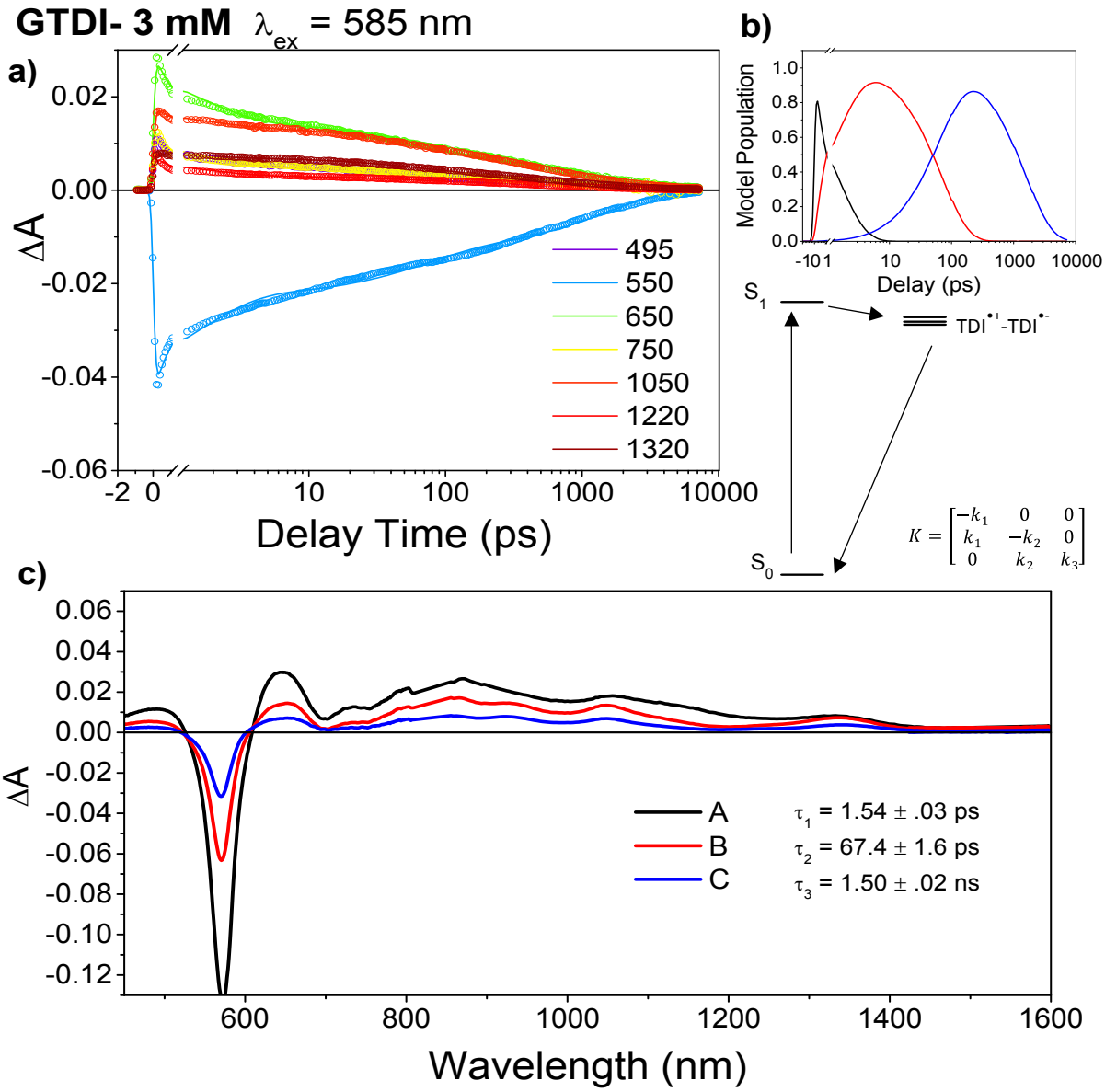

Figure S11: fsTA analysis of **GTDI** in 3 x 10^{-3} M THF. a) Kinetic data and overlaid fit at selected wavelengths, b) model population c) species-associated spectra.

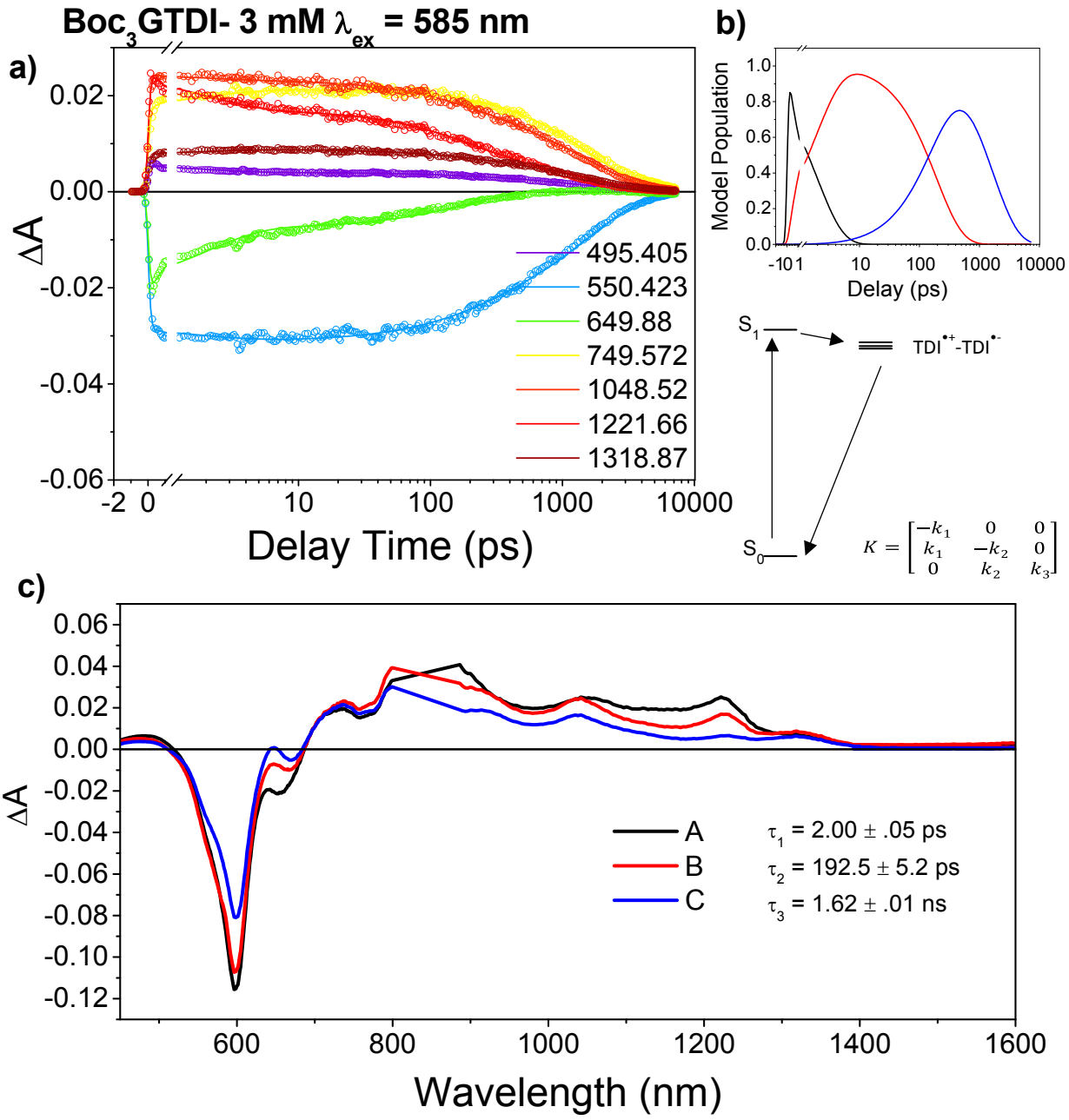

Figure S12: fsTA analysis of Boc_3GTDI in 3 x 10^{-3} M THF. a) Kinetic data and overlaid fit at selected wavelengths, b) model population c) species-associated spectra.

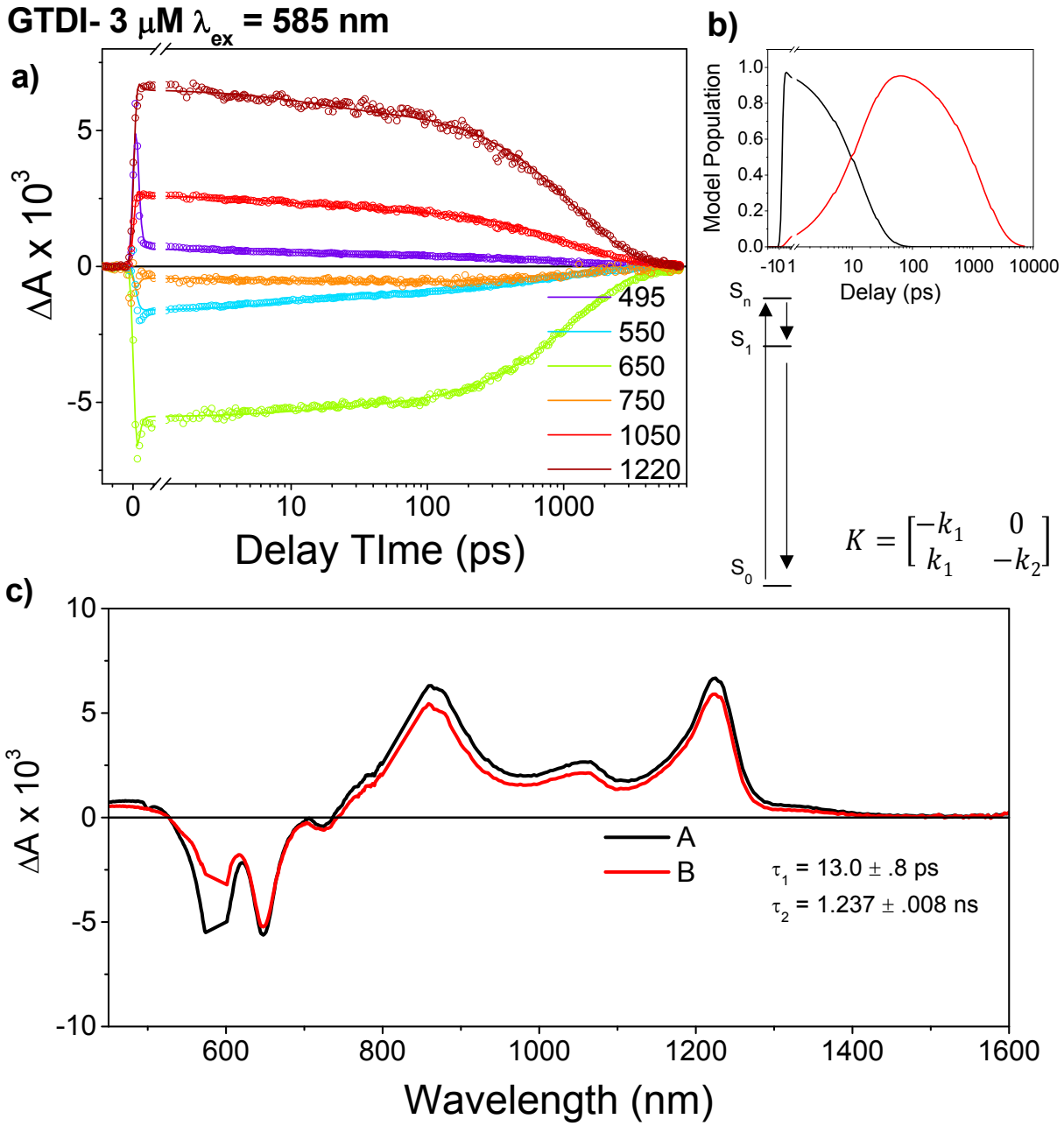

Figure S13: fsTA analysis of **GTDI** in 3 x 10^{-6} M THF. a) Kinetic data and overlaid fit at selected wavelengths, b) model population c) species-associated spectra.

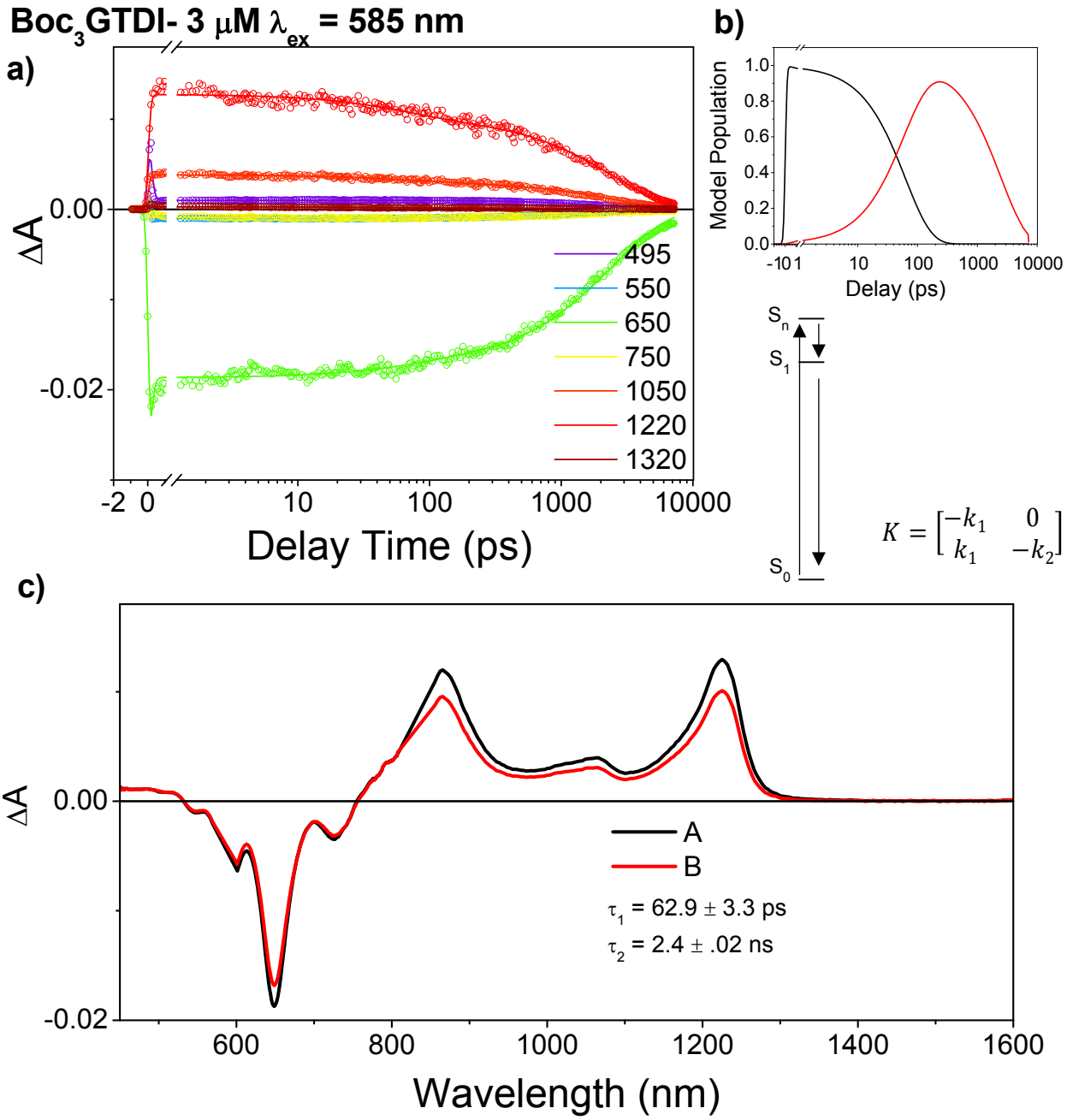

Figure S14: fsTA analysis of **Boc_3GTDI** in 3 x 10^{-6} M THF. a) Kinetic data and overlaid fit at selected wavelengths, b) model population c) species-associated spectra.

Triplet Sensitization of GTDI

Triplet sensitization of GTDI was performed in a 3 x 10^{-4} M solution of THF by photoexcitation of anthracene (in large excess) at 355 nm. Rapid intersystem crossing populates the anthracene T_1 state (1.85 eV); the anthracene T_1 state triplet energy transfers to the lower energy TDI T_1, which allows for optical characterization of the TDI T_1 state by nanosecond transient absorption spectroscopy. The sample was prepared in airfree conditions.

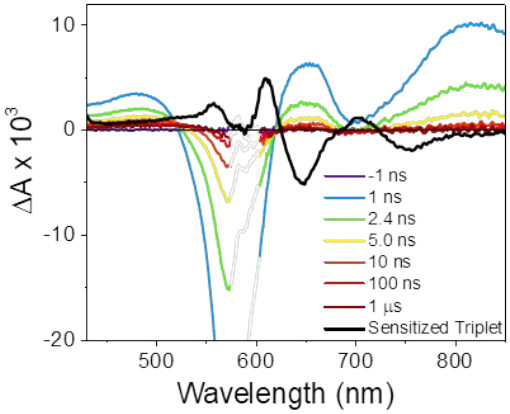

Figure S15: Selected time traces of 3 x 10^{-4} M GTDI in THF (λ_{ex} = 590 nm), overlaid with sensitized triplet spectrum.

Excitation-Dependent fsTA Spectroscopy

Samples of concentrated GTDI were excited at 590 nm and 670 nm to probe for the existence of a CT state in the steady state absorption. Overlays of spectra at selected delay times display minimal change between excitation energies. Plotting the delay traces for wavelengths associated with the TDI anion band reveals an initial fast relaxation at 650 nm after higher energy excitation, likely due to cooling from a higher lying vibrational state.

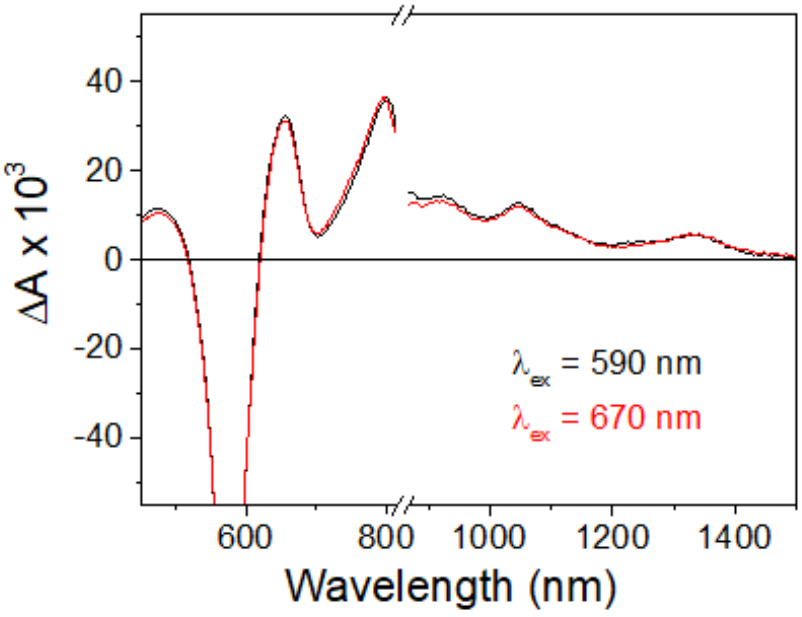

Figure S16: Spectra of (~10^{-3}) M GTDI in THF at 10 ps following excitation at 590 nm (black) and 670 nm (red).

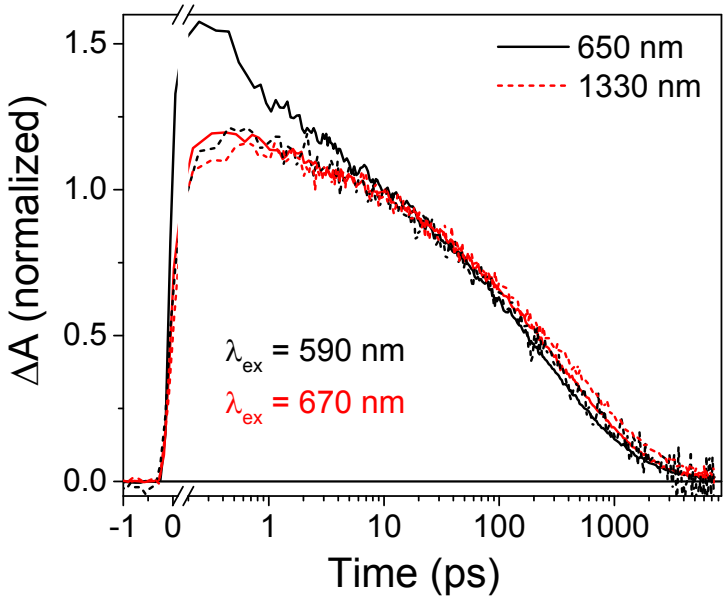

Figure S17: Delay traces of selected wavelengths of GTDI excited at 590 nm (black) and 670 nm. Traces were normalized to the intensity at 10 ps.

Femtosecond Infrared Absorption (fsIR) Spectroscopy

The femtosecond transient IR (fsIR) spectroscopy apparatus has also been previously described.[9]

Upon photoexcitation λ_{ex} = 590 nm (4 mϑ/pulse), **GTDI** displays an absorption at 1564 cm^{-1}, close to the reported 1572 cm^{-1} mode for $TDI^{\bullet-}$ anion. **Boc_3GTDI** also display this feature, but displays and additional sharp feature at 1665 cm^{-1}, in line with features reported for the singlet excited state of TDI.

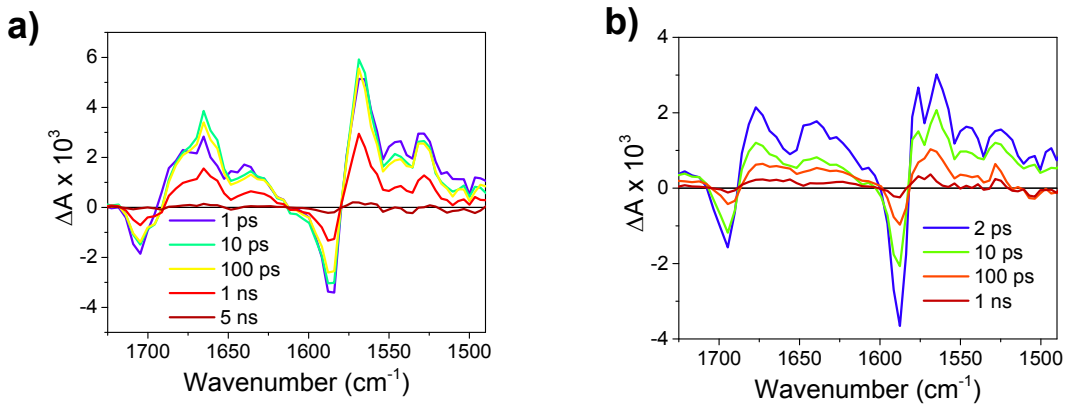

Figure S18: fsIR spectra of **GTDI** and **Boc_3GTDI** (3 x 10^{-3} M) at various delay times.

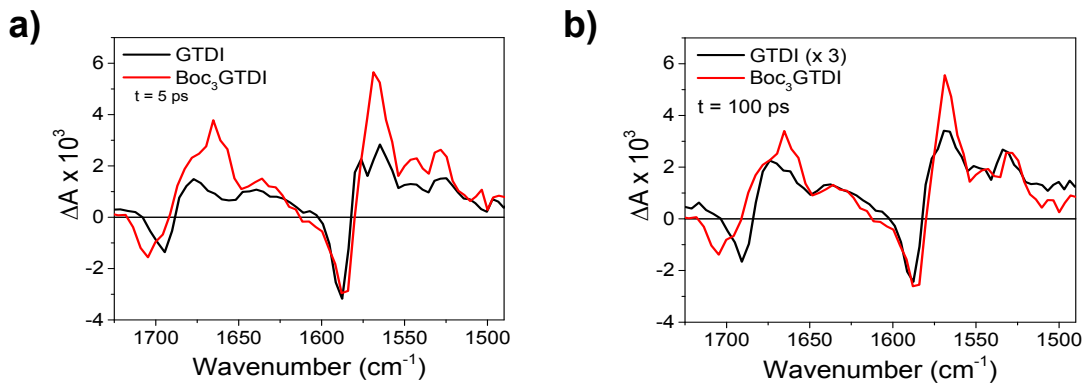

Figure S19: fsIR spectra of **GTDI** and **Boc$_3$GTDI** following a excitation pulse of 590 nm at a delay time of a) 5 ps, and b) 100 ps.

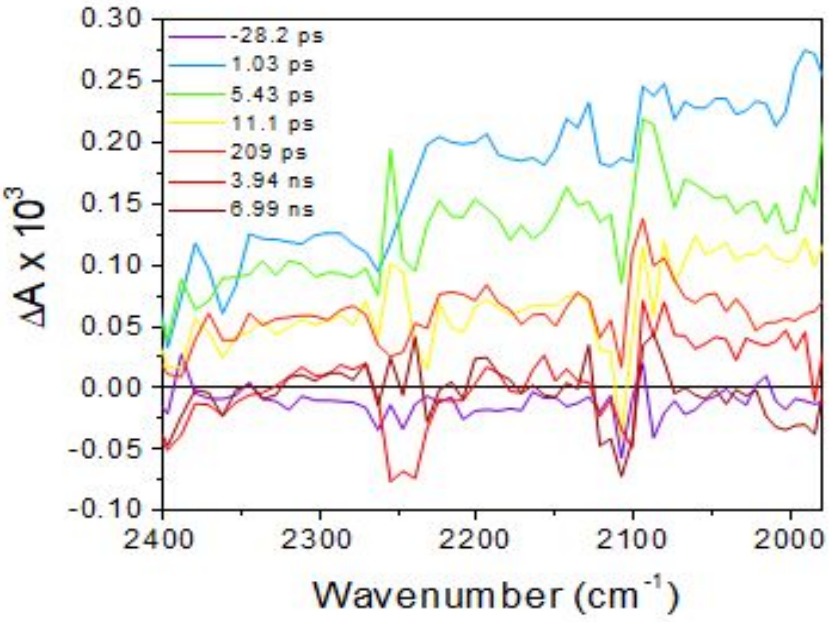

Figure S20: fsIR spectra of **GTDI** following excitation pulse of 590 nm at various delay times.

References

1. Wu, Y.-L.; Horwitz, N. E.; Chen, K.-S.; Gomez-Gualdron, D. A.; Luu, N. S.; Ma, L.; Wang, T. C.; Hersam, M. C.; Hupp, J. T.; Farha, O. K.; Snurr, R. Q.; Wasielewski, M. R., G-quadruplex organic frameworks. *Nat. Chem.* **2016,** *9*, 466.
2. Franke, D.; Petoukhov, M. V.; Konarev, P. V.; Panjkovich, A.; Tuukkanen, A.; Mertens, H. D. T.; Kikhney, A. G.; Hajizadeh, N. R.; Franklin, J. M.; Jeffries, C. M.; Svergun, D. I., Atsas 2.8: A comprehensive data analysis suite for small-angle scattering from macromolecular solutions. *J. Appl. Cryst.*. **2017,** *50* (4), 1212-1225.
3. Hanwell, M. D.; Curtis, D. E.; Lonie, D. C.; Vandermeersch, T.; Zurek, E.; Hutchison, G. R., Avogadro: An advanced semantic chemical editor, visualization, and analysis platform. *J. Cheminformatics* **2012,** *4* (1), 17.
4. Svergun, D.; Barberato, C.; Koch, M. H. J., Crysol - a program to evaluate x-ray solution scattering of biological macromolecules from atomic coordinates. *J. Appl. Cryst.* **1995,** *28* (6), 768-773.
5. Chen, M.; Bae, Y. J.; Mauck, C. M.; Mandal, A.; Young, R. M.; Wasielewski, M. R., Singlet fission in covalent terrylenediimide dimers: Probing the nature of the multiexciton state using femtosecond mid-infrared spectroscopy. *J. Am. Chem. Soc.* **2018,** *140* (29), 9184-9192.
6. Young, R. M.; Dyar, S. M.; Barnes, J. C.; Juricek, M.; Stoddart, J. F.; Co, D. T.; Wasielewski, M. R., Ultrafast conformational dynamics of electron transfer in exbox4+⊂perylene. *J. Phys. Chem. A* **2013,** *117* (47), 12438-12448.
7. The MathWorks, I., Natick, Massachusetts, United States.
8. Berberan-Santos, M. N.; Martinho, J. M. G., The integration of kinetic rate equations by matrix methods. *J. Chem. Ed.* **1990,** *67* (5), 375.
9. Mauck, C. M.; Young, R. M.; Wasielewski, M. R., Characterization of excimer relaxation via femtosecond shortwave- and mid-infrared spectroscopy. *J. Phys. Chem. A* **2017,** *121* (4), 784-792.